Vascular Pharmacology 100 (2018) 34–40

Contents lists available at ScienceDirect

Vascular Pharmacology

journal homepage: www.elsevier.com/locate/vph

Axitinib attenuates intraplaque angiogenesis, haemorrhages and plaque destabilization in mice

Bieke Van der Veken, Guido R.Y. De Meyer, Wim Martinet*

Laboratory of Physiopharmacology, University of Antwerp, Belgium

ARTICLE INFO

Keywords:
Atherosclerosis
Plaque stability
Intraplaque neovascularization
Angiogenesis
Mouse model

ABSTRACT

Aim: An increased density of intraplaque (IP) microvessels in ruptured versus nonruptured human plaques suggests that IP neovascularization has a major causative effect on plaque development and instability. Possibly, vascular endothelial growth factor (VEGF) or other angiogenic factors mediate IP microvessel growth and plaque destabilization. Because apolipoprotein deficient mice with a heterozygous mutation (C1039G +/−) in the fibrillin-1 gene ($ApoE^{-/-}Fbn1^{C1039G+/-}$) manifest substantial IP neovascularization, they represent a unique tool to further investigate angiogenesis and its role in atherosclerosis. Here, we examined whether administration of axitinib (inhibitor of VEGF receptor-1,-2 and -3) inhibits IP neovascularization and stabilizes atherosclerotic plaques.

Methods: $ApoE^{-/-}Fbn1^{C1039G+/-}$ mice were fed a western diet (WD) for 20 weeks. After 14 weeks WD, mice received axitinib (35 μg/g) or solvent i.p. 4 ×/week for 6 weeks. Cardiac function was monitored to evaluate the effect of axitinib on atherosclerosis-driven complications such as myocardial infarction.

Results: Axitinib significantly reduced IP neovascularization, with subsequent less prevalence of IP haemorrhages. The smooth muscle cell content doubled, whereas the amount of macrophages decreased. Overall cardiac function was improved in axitinib-treated animals. Moreover, the number of animals with myocardial infarction was decreased by 40%. Coronary plaque formation was observed in almost all control animals whereas treated animals showed a 30% reduction in the occurrence of coronary plaques.

Conclusions: Inhibition of VEGF receptor signalling by axitinib attenuates intraplaque angiogenesis and plaque destabilization in mice.

1. Introduction

Rupture of atherosclerotic plaques and the subsequent formation of thrombi are the most prevalent causes of clinical complications in atherosclerosis and lead to a tremendously high mortality rate [1]. A growing body of evidence indicates that intraplaque (IP) neovascularization is a critical factor stimulating plaque rupture [2,3]. Indeed, human vulnerable lesions are characterized by a structured web of IP microvessels that originate from the vasa vasorum and that grow through the media into the plaque. In rare cases, IP microvessels are also sprouting from the luminal side of the vessel wall. Hypoxia is the primary stimulus of IP angiogenesis and may arise due to plaque expansion and increased plaque inflammation [4]. The development of a network of IP microvessels is essential for a continuous supply of oxygen and nutrients into the growing plaque, with inflammatory mediators claiming the majority of the increased energy demand [5,6]. Importantly, due to an imbalance in pro-angiogenic factors (e.g. vascular endothelial growth factor (VEGF), angiopoietin [Ang] 2) and pro-maturation factors (e.g. platelet-derived growth factor (PDGF), angiopoietin [Ang] 1) inside the plaque, IP microvessels are characterized by open tight junctions, detachment of the basement membrane and poor coverage with pericytes, indicating that IP microvessels are extremely fragile and immature [7]. The immaturity of IP microvessels promotes extravasation of lipids, inflammatory mediators and erythrocytes in the plaque, and thus may advance plaque progression and rupture [8–10].

Throughout the years, scientific knowledge on the significance of IP neovascularization in plaque stability was mainly acquired through human specimens. The absence of a decent animal model of plaque rupture hampered the development of therapeutic strategies with IP microvessels as a valuable target. Recently, a unique model of spontaneous plaque rupture has been introduced, namely the $ApoE^{-/-}$ Fibrillin $(Fbn)1^{C1039G+/-}$ mouse. The heterozygous mutation $C1039G^{+/-}$ in the Fbn1 gene results in fragmentation of elastic fibres in the media of the vessel wall [11]. Combined with a western-type diet, degradation of elastic fibres leads to enhanced plaque formation in $ApoE^{-/-}$ mice with typical features of human unstable lesions

* Corresponding author.
E-mail address: Wim.Martinet@uantwerpen.be (W. Martinet).

http://dx.doi.org/10.1016/j.vph.2017.10.004
Received 9 June 2017; Received in revised form 4 October 2017; Accepted 19 October 2017
Available online 31 October 2017

including IP neovascularization and haemorrhages. This mouse model also reveals sporadic plaque rupture and myocardial infarction without any mechanical intervention [12]. Accordingly, ApoE$^{-/-}$ Fbn $1^{C1039G+/-}$ mice are an ideal tool to investigate whether inhibition of IP neovascularization and thus a reduction in the amount of microvessels promotes plaque stability.

VEGF (with VEGFR-2 as its main receptor) is a main challenger during IP neovascularization [13]. VEGFRs are tyrosine kinases that autophosphorylate their intracellular tyrosine residues upon activation. Low levels of VEGF-A are important for vascular homeostasis, though at higher levels, VEGF-A initiates vascular endothelial cell (EC) proliferation/migration and increases vascular permeability, thereby inducing neovascularization [14]. These insights offer new possibilities in plaque stabilization through the inhibition of VEGF signalling [15]. In cancer research, VEGF-inhibiting therapies have proven their potential, however, in atherosclerosis research the success of this approach remains to be elucidated. Patients receiving VEGF-inhibiting medication can experience cardiovascular side effects such as high blood pressure and a slight increase (1%) in the occurrence of myocardial infarctions [16].

In this study, ApoE$^{-/-}$ Fbn1$^{C1039G+/-}$ mice were treated with axitinib, a drug that selectively inhibits VEGFR-1, -2 and -3 at subnanomolar concentrations, in order to unravel the impact of diminished IP neovascularisation on plaque destabilization and subsequent clinical complications.

2. Materials and methods

2.1. Mice

Female ApoE$^{-/-}$ Fbn1$^{C1039G+/-}$ mice were fed a Western diet (WD) (AB diets, Woerden, the Netherlands) starting at an age of 8 weeks [11,12]. The animals were housed in a temperature-controlled room with a 12 h light/dark cycle and had free access to water and food. Cases of sudden death were documented. Because IP microvessels are already developing at 14WD in ApoE$^{-/-}$ Fbn1$^{C1039G+/-}$ mice, this time point was chosen to start the treatment. Mice were treated with axitinib (35 mg/kg, i.p., 4 ×/week) for 6 weeks. Axitinib (kindly provided by Pfizer Inc., New York, USA) was dissolved in 3 parts of polyethylene glycol 400 and 7 parts of water with pH 2–3 to prevent precipitation. Control mice received PEG400/H_2O injections in the same frequency as the treated group. At the end of the experiment (20 weeks WD), blood samples were obtained from the retro-orbital plexus of anesthetised mice (sodium pentobarbital 75 mg/kg, i.p.). Subsequently, mice were sacrificed with sodium pentobarbital (250 mg/kg, i.p.). Analysis of total plasma cholesterol was performed via a commercially available kit (Randox laboratories, Crumlin, UK). All animal procedures were conducted according to the guidelines from Directive 2010/63/EU of the European Parliament on the protection of animals used for scientific purposes. Experiments were approved by the ethics committee of the University of Antwerp.

2.2. Histology

After sacrifice of ApoE$^{-/-}$ Fbn1$^{C1039G+/-}$ mice, the proximal aorta, aortic arch, carotid artery and heart were collected. Tissues were fixed in 4% formalin for 24 h, dehydrated overnight in 60% isopropanol and subsequently embedded in paraffin. Serial longitudinal sections (4 μm) of the carotid arteries and aortic arch were cut and prepared for histological analysis. Cross-sections (4 μm) were cut from the proximal aorta and heart. Haematoxylin-eosin (HE) staining was performed to analyse the plaque size, plaque thickness and necrotic core. The plaque thickness was assessed by taking the mean value of 10 random measurements in the respective area. The plaque formation index was calculated on longitudinal sections by using the following formula [(Σ total plaque length / Σ total vessel length) × 100]. Necrosis was defined as acellular areas filled with necrotic clefts and necrotic debris. Immunohistochemical stainings for CD31 (anti-CD31, PC054, Binding Site, Birmingham, UK) and Ter-119 (anti-Ter-119, 550,565, BD Biosciences, USA) were performed to detect plaque ECs and erythrocytes, respectively. The analysis of IP microvessels and IP haemorrhages was done as follows. Fifteen consecutive slices were cut from the paraffin-embedded tissue. In every tissue slice, the amount of microvessels and haemorrhages in the plaques were counted per area. A mean value was calculated as a representative value for the amount of IP microvessels and haemorrhages per area (per vessel). Plaque composition was analysed with a Sirius red and anti-α-SM actin (A2547, Sigma, UK) staining to detect collagen and smooth muscle cells. Collagen type I and III was quantified under polarized light. Macrophages were detected by immunohistochemistry using an anti-Monocyte/Macrophage (553,322, Pharmingen, San Diego, CA) or anti-MAC3 (550,292, Pharmingen, San Diego, CA) staining. The hypoxic area was measured using pimonidazole (HP1-1000kit, hypoxyprobe, Massachussets, USA) [5]. The occurrence of myocardial infarctions (defined as large fibrotic areas) and coronary plaques was analysed on Masson's trichrome staining (transversal sections).

2.3. Echocardiography

Transthoracic echocardiograms were performed on anesthetized mice (isoflurane, 4% for induction and 2.5% for maintenance) at the end of the experiment using a VEVO2100 (VisualSonics, Toronto, Canada), equipped with a 25 MHz transducer. The left ventricular internal diameter during diastole (LVIDd) and left ventricular internal diameter during systole (LVIDs) were measured and fractional shortening [FS = (LVIDd − LVIDs) / LVIDd × 100] was calculated.

2.4. Blood pressure measurements

Peripheral blood pressure was measured at week 20 before sacrifice in conscious mice via a tail cuff. Mice were placed in plexiglas restrainers in a heating chamber (37 °C) and kept in the dark. Ten minutes of acclimatization was allowed before measurements were initiated. At the distal end of the tail, a pulse sensor and occluding cuff controlled by a programmed Electro-Sphygmomanometer (Narco Bio-systems, Austin, TX) were placed. Voltage output from the sensor and cuff were recorded and analysed by a PowerLab signal transduction unit and associated Chart software (ADInstruments, Colorado Springs, CO). To be accustomed to the procedure, mice were trained for 4 weeks before the first measurement.

2.5. Elisa

An enzyme-linked immunosorbent assay for quantitative detection of mouse VEGF-A (BMS619/2, eBioscience, San Diego, USA) was performed to detect VEGF-A in the plasma of control and treated mice.

2.6. Cell culture

Human umbilical vein endothelial cells (HUVECs) were cultured in M199 medium supplemented with 20% fetal bovine serum, 1% non-essential amino-acids and antibiotics. To investigate the expression of adhesion molecules or VE-cadherin, HUVECs were treated with 10 ng/ml human TNF-α (hTNF-α) in the presence or absence of axitinib (100 nM). After 24 h, cells were lysed to perform qPCR. Total RNA was isolated using an Isolation II RNA mini kit (BIO-52073, Bioline, Taunton, USA) according to the manufacturer's instructions. Reverse transcription was performed with a sensifast™ cDNA Synthesis Kit (BIO-65053, Bioline, Taunton, USA). Thereafter, Taqman gene expressions assays for VCAM-1 (Hs01003372_m1), ICAM-1 (Hs00164932_m1), *E*-selectin (Hs00204397_m1) and VE-cadherin (Hs00170986_m1) were performed in duplicate on an ABI-prism 7300 sequence detector system

(Applied Biosystems, California, USA). The parameters for PCR amplification were 95 °C for 10 min followed by 10 cycles of 95 °C for 15 s and 60 °C for 1 min. Relative expression of mRNA was calculated using the comparative threshold cycle method. All data were normalized for quantity cDNA input by performing measurements on the endogenous reference gene β-actin.

2.7. Statistics

All data are expressed as mean ± SEM. Statistical analyses were performed using SPSS software (version 23, SPSS Inc., Chicago, IL). Statistical tests are specified in the figure and table legends. Differences were considered significant at $p \leq 0.05$.

3. Results

3.1. Axitinib inhibits intraplaque neovascularization

Axitinib significantly lowered VEGF-A levels in the plasma of mice (ctrl 2344 ± 745 pg/ml vs axitinib 757 ± 277 pg/ml, p = 0.0392). CD31 staining of atherosclerotic plaques in treated mice revealed a significantly lower number of microvessels, both in the aortic arch (AA) and right common carotid artery (RCCA), as compared to plaques from untreated controls (Fig. 1A and B), yet the reduction in IP neovascularization was more pronounced in the AA. Microvessels were primarily sprouting from the media into the plaque. Anti-Ter-119 immunostainings of the AA and RCCA showed a significantly reduced level of IP haemorrhages in treated versus untreated animals (Fig. 1A and B). Moreover, the number of mice displaying IP haemorrhages was significantly higher in control animals as compared to treated animals (AA: control = 73%; axitinib = 10%, p = 0.015; RCCA: control = 83%; axitinib = 43%, p = 0.126, Fisher's exact test). Microvessels stained negative for α-SM actin (data not shown), suggesting that they were not fully matured. Hypoxia in the plaque, as determined via a pimonidazole staining, was significantly lower in the proximal aorta (0.40 ± 0.13% positivity) as compared to the AA (4.60 ± 1.70%, p = 0.029) and RCCA (5.12 ± 1.42%, p = 0.012). In respect to the latter finding, IP neovascularization did not occur in the proximal aorta.

3.2. Axitinib promotes plaque stability without affecting plaque thickness

The mean plaque thickness and necrotic core area in plaques of the AA and RCCA was not changed (Table 1), although total plasma cholesterol was significantly reduced after treatment with axitinib (control 547 ± 38 mg/dl, axitinib 412 ± 29 mg/dl, p = 0.019, Independent samples *t*-test, n = 10–14). Body weight was similar between control (20.2 ± 0.7 g) and treated (20.8 ± 0.2 g) animals. The plaque formation index was significantly decreased in the RCCA and tended to decrease in the AA (Table 1). Plaque composition was clearly different between both groups. In both the AA and RCCA, axitinib-treated mice presented a plaque phenotype with significantly more smooth muscle cells (SMCs), whereas the macrophage content was significantly decreased (Table 1). The percentage of total collagen as well as collagen type I and type III in plaques of the AA did not differ (data not shown). In the RCCA, total collagen was significantly increased in axitinib-treated animals (Table 1). In the proximal aorta, where IP neovascularization did not occur, no significant change could be observed in plaque size and composition (Table 1).

3.3. Axitinib reduces the expression of adhesion molecules in vitro and improves the endothelial barrier

To investigate whether the reduced plaque formation is associated with changes in the expression levels of adhesion molecules or VE-cadherin, HUVECs were stimulated with hTNF-α in the presence or absence of axitinib (100 nM). After 24 h, treatment of HUVECs with hTNF-α and axitinib resulted in a significant decrease in mRNA expression relative to β-actin of the adhesion markers VCAM-1 (ctrl: 1.11 ± 0.03 axitinib: 0.90 ± 0.02, p = 0.0003), ICAM-1 (ctrl:

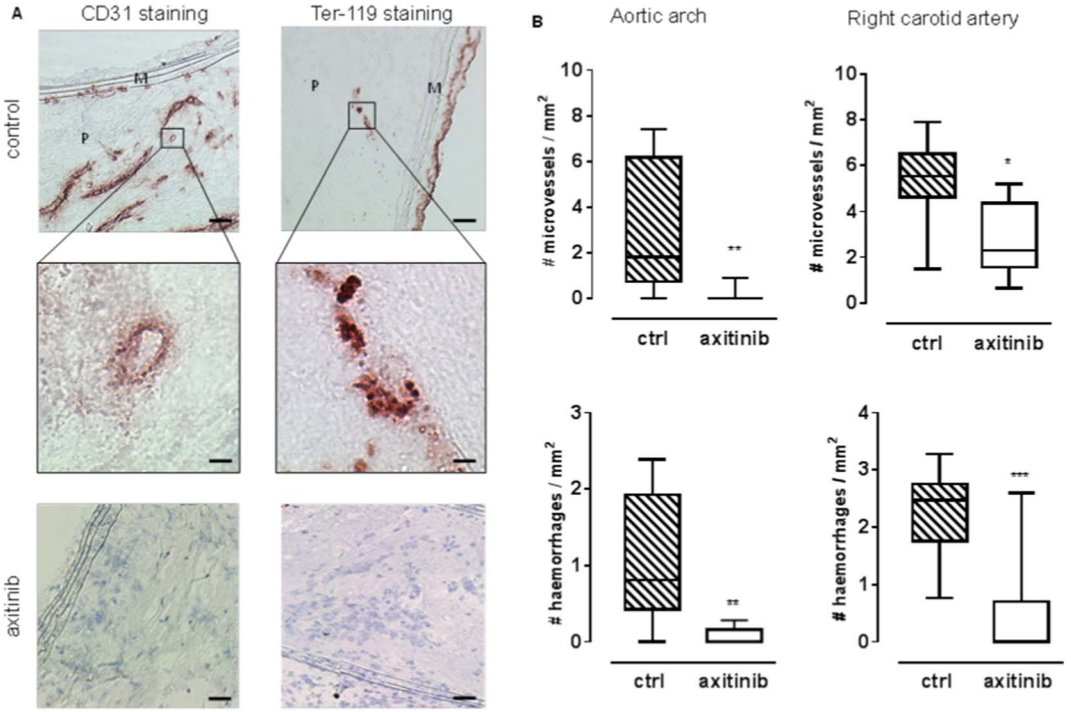

Fig. 1. Axitinib inhibits intraplaque neovascularization in the aortic arch and carotid artery of ApoE$^{-/-}$Fbn1$^{C1039G+/-}$ mice. (A) Representative images of a CD31 and Ter-119 staining to detect IP microvessels and IP haemorrhages, respectively, in atherosclerotic plaques of control and axitinib-treated mice. Scale bar = 50 μm or 0.5 μm (boxed area). M = media, P = plaque. (B) Quantification of IP microvessels and IP haemorrhages in the aortic arch and right carotid artery of control and axitinib-treated mice. (Control n = 8, axitinib n = 9, Mann-Whitney *U* test; *p < 0.05, **p < 0.01, ***p < 0.001).

Table 1
Plaque thickness and composition in the aortic arch, carotid artery and proximal aorta of ApoE$^{-/-}$ Fbn1$^{C1039G+/-}$ mice.

	Arteries with IP microvessels				Arteries without IP microvessels	
	Aortic arch		Carotid artery		Proximal ascending aorta	
	Control	Axitinib	Control	Axitinib	Control	Axitinib
Plaque thickness (μm)	340 ± 41	407 ± 52	293 ± 19	266 ± 20	262 ± 23	284 ± 20
Plaque formation index (%)	89 ± 4	79 ± 6	88 ± 5	64 ± 7*	n.d.	n.d.
Necrotic core area (10^3 μm^2)	84 ± 11	93 ± 20	58 ± 16	86 ± 26	39 ± 10	35 ± 7
Collagen (%)	9.0 ± 1.7	11.2 ± 2.1	31.7 ± 2.1	37.6 ± 1.7*	7.7 ± 1.6	9.8 ± 1.0
Smooth muscle cells (%)	5.0 ± 0.8	9.7 ± 0.8***	3.4 ± 0.5	7.9 ± 1.2*	12.5 ± 1.5	13.0 ± 0.8
Macrophages (%)	8.4 ± 1.6	4.4 ± 0.9*	8.8 ± 0.8	5.7 ± 1.0*	5.0 ± 0.5	5.1 ± 0.7

Data shown as mean ± SEM, n = 10–16, independent samples *t*-test; n.d. = not determined (cross-sections of the proximal aorta were cut, which excluded the possibility of measuring the plaque formation index).
* $p < 0.05$.
*** $p < 0.001$.

1.08 ± 0.03 axitinib: 0.93 ± 0.05, p = 0.0199) and E-selectin (ctrl: 1.27 ± 0.04 axitinib: 0.79 ± 0.02, p < 0.0001) as compared to the control group. Expression of VE-cadherin was significantly higher in HUVECs treated with axitinib relative to β-actin (ctrl: 1.07 ± 0.43 axitinib: 0.94 ± 0.04, p = 0.0270).

3.4. Axitinib improves cardiac function and morphology

We previously reported that ApoE$^{-/-}$ Fbn1$^{C1039G+/-}$ mice spontaneously develop myocardial infarctions on a western type diet [12]. Given the importance of neovascularization to restore perfusion to the ischemic myocardium after an acute myocardial infarction, we assessed cardiac function and structure after axitinib treatment via echocardiography and histology. LVIDd (control = 4.6 ± 0.2 mm; axitinib = 4.1 ± 0.2 mm, p = 0.02) and LVIDs (control = 3.6 ± 0.2 mm; axitinib = 2.9 ± 0.2 mm, p = 0.04) were significantly smaller as compared to control mice, resulting in an increased level of FS (Fig. 2A). Moreover, a significant reduction in HW/BW was observed in treated animals as compared to the control group (Fig. 2B). To confirm this reduction in heart weight, left ventricular (LV) mass and cardiomyocyte size were analysed. Both parameters were significantly decreased in the axitinib-treated group (Fig. 2C and D). Analysis of fibrotic areas on heart sections showed a significant decrease in the occurrence of myocardial infarction (MI) after treatment (Fisher's exact test, p = 0.05, Fig. 3A, B, D). The infarct size was not different after treatment with axitinib (control = 3.8 ± 1.8 mm^2 vs axitinib = 3.1 ± 1.6 mm^2, p = 0.77). Coronary plaque formation was observed in almost all control animals whereas axitinib-treated animals showed a 30% reduction in the occurrence of coronary plaques (Fig. 3C). Axitinib did not affect systolic blood pressure (control = 90 ± 5 mmHg; axitinib = 89 ± 5 mmHg, p = 0.90), diastolic blood pressure (control = 56 ± 4 mmHg; axitinib = 61 ± 5 mmHg, p = 0.51) or mean pressure (control = 67 ± 4 mmHg; axitinib = 70 ± 5 mmHg, p = 0.70).

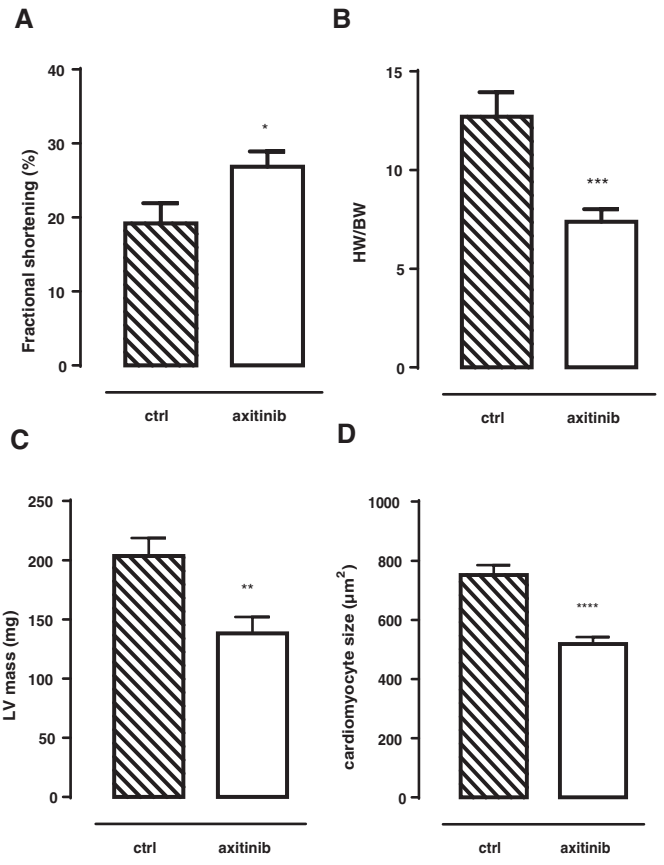

Fig. 2. Axitinib improves cardiac morphology and function in ApoE$^{-/-}$ Fbn1$^{C1039G+/-}$ mice. Fractional shortening as a measure of cardiac function (A) as well as heart weight (HW) divided by body weight (BW) (B), left ventricular mass (C) and cardiomyocyte size (D) in control mice versus axitinib-treated mice are shown. (Control n = 13, axitinib n = 13, Independent samples *t*-test; *p < 0.05, **p < 0.01, ***p < 0.001).

4. Discussion

Although IP neovascularization plays a significant role in atherosclerotic plaque destabilization and rupture because of the additional supply of lipids and inflammatory mediators to the lesion [2], the potential of IP neovascularization as a novel therapeutic target remained mostly unexplored due to the lack of a decent animal model of plaque rupture. However, recent evidence indicates that atherosclerotic plaques in ApoE$^{-/-}$ Fbn1$^{C1039G+/-}$ mice display striking similarities with complex human atherosclerotic lesions including presence of IP neovascularization and haemorrhages [12], which makes this mouse a unique model for investigating crucial aspects of plaque destabilization. In the present study, we provide evidence that VEGF in ApoE$^{-/-}$ Fbn1$^{C1039G+/-}$ mice exerts a key role in IP neovascularization and thus in plaque destabilization. Indeed, inhibition of VEGFR signalling by the selective VEGFR inhibitor axitinib significantly reduced IP neovascularization and haemorrhages both in the aortic arch (AA) and right common carotid artery (RCCA), as compared to plaques from untreated controls. However, the maturation of resting neovessels was not affected by axitinib and therefore these neovessels remained 'leaky'.

Given the promising findings described above, we next examined the effect of axitinib on plaque size and composition. Plaque thickness was similar in controls and axitinib-treated animals. Nevertheless, axitinib-treated plaques, at least in the RCCA, showed a more stable

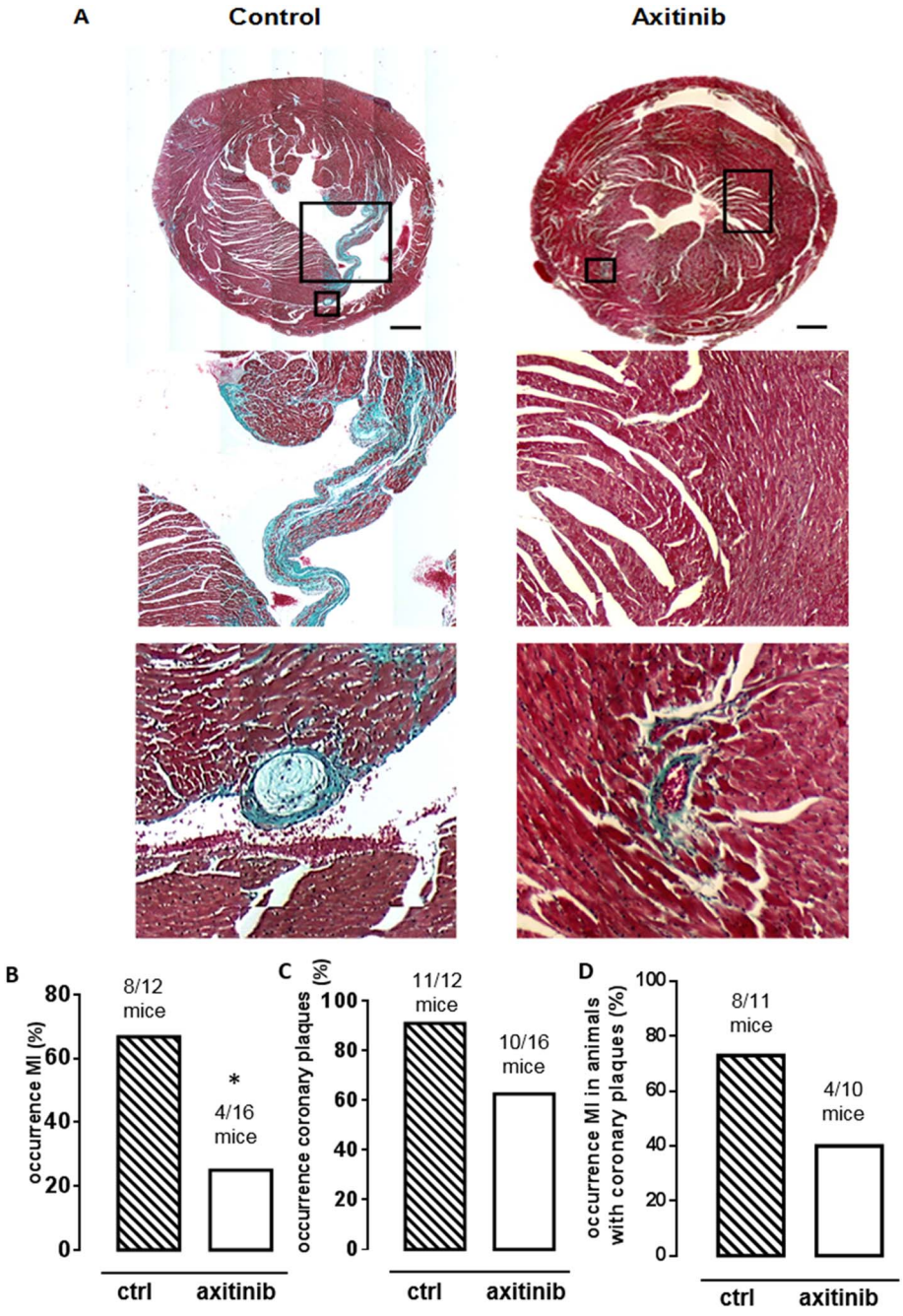

Fig. 3. Axitinib attenuates the occurrence of myocardial infarction and coronary plaque formation in ApoE$^{-/-}$Fbn1$^{C1039G+/-}$ mice. (A) Trichrome Masson staining of heart tissue revealing large infarcted areas with coronary plaque formation in control ApoE$^{-/-}$Fbn1$^{C1039G+/-}$ mice as compared to treated mice. Scale bar = 200 μm. Magnifications of the boxed areas (illustrating the infarction zone and coronary plaque formation) are shown. (B–D) Number of mice with a myocardial infarction (B, $p = 0.05$), coronary plaque formation (C, $p = 0.18$) and with a myocardial infarction in the presence of coronary plaques (D, $p = 0.19$). (Control n = 9, axitinib n = 10, Fisher's exact test).

plaque phenotype as demonstrated by increased levels of SMCs and total collagen, whereas the macrophage content decreased. Because entry of monocytes and macrophages is related to leakage of neovessels, a reduction in the amount of macrophages may be a direct result of the decreased neovessel network in the plaque. Indeed, arteries without IP neovascularization such as the proximal aorta did not reveal a decrease in macrophage content after axitinib treatment and had similar plaque stability as compared to control animals. As shown previously by Sluimer and Daemen [6], the degree of hypoxia in the proximal aorta is significantly lower than in the RCCA and AA, which may explain why plaques in the proximal aorta do not develop IP microvessels. Probably, a threshold of hypoxia needs to be trespassed before IP neovascularization occurs in ApoE$^{-/-}$Fbn1$^{C1039G+/-}$ mice. However, mice that do not reveal a detectable number of IP microvessels in the RCCA also had lower amounts of macrophages after treatment with axitinib, suggesting that the decrease in macrophages is not solely due to a reduced amount of microvessels, but also due to other mechanisms. Indeed, it is known that VEGF has a distinct effect on monocyte activation/chemotaxis and the upregulation of matrix metalloproteinases [17,18]. Moreover, even though the plaque size of axitinib-treated mice remained unchanged, longitudinal sections of the RCCA and AA revealed that axitinib decreased plaque formation, which points towards a more important role for VEGFR signalling in early atherogenesis. In general, when ECs undergo inflammatory activation, the upregulation of adhesion molecules such as ICAM-1 and VCAM-1 represent an important trigger in early lesion development, as they attract and encourage monocytes to enter the lesion. In the present study, we provide in vitro evidence that axitinib interferes with the upregulation of adhesion molecules. HUVECs pre-activated with TNF-α and treated with axitinib showed decreased levels of the adhesion molecules VCAM-1 and ICAM-1 as well as E-selectin, which are all involved in plaque development. In addition, expression of VE-cadherin was stimulated by axitinib, which

suggests that axitinib can impair the subendothelial invasion of LDL. Finally, it is noteworthy that total plasma cholesterol decreased by 25% after axitinib treatment. Even though plasma cholesterol levels were still relatively high (> 400 mg/dl) and such a drop in plasma cholesterol did not affect plaques in the proximal aorta without IP neovascularization, we cannot rule out that the observed changes in plaque composition are partially due to a decrease in plasma cholesterol. In literature, no significant effects of axitinib on total plasma cholesterol were reported. However, Heinonen et al. [19] observed alterations in lipid profiles and plasma lipid levels, induced by alterations in VEGF-A. These lipid alterations are linked to a reduction in plasma lipoprotein lipase (LPL) activity in response to an increase in VEGF-A. Given that axitinib significantly lowered VEGF in plasma of $ApoE^{-/-}Fbn1^{C1039G+/-}$ mice, an increase in LPL may result in a decreased level of total plasma cholesterol.

Our findings are in line with previous reports from other groups showing that administration of VEGF protein promotes plaque development [19,20], while vaccination against VEGFR-2 attenuates atherogenesis [21]. Interestingly, vein grafts in hypercholesterolemic ApoE*3 Leiden mice represent an alternative, yet useful model for IP microvessel research [22]. Inhibition of VEGFR-2 signalling in vein graft lesions by VEGFR-2 blocking antibodies (DC101) reduced IP haemorrhages, but did not affect endothelial cell growth as the number of microvessels was equal in DC101-treated mice and untreated controls [22,23]. It should be noted that DC101 antibodies target only VEGFR-2 whereas axitinib inhibits VEGFR-1, VEGFR-2 and VEGFR-3. Because VEGFR-1 and VEGFR-3 can contribute to pathological angiogenesis in certain conditions [24,25], combined inhibition of VEGFR-1, VEGFR-2 and VEGFR-3 may lead to a more pronounced result yielding a reduced IP microvessel network. Some findings in literature seem to be inconsistent with the present results at first sight. Indeed, gene transfer of VEGF had no significant impact on atherosclerotic plaque formation and stability in $ApoE^{-/-}$ mice [26], whereas administration of a pan-VEGFR inhibitor resulted in increased plaque size and plaque vulnerability [27]. Two aspects of VEGFR signalling should be highlighted to explain these illusory discrepancies. First, VEGF plasma levels were not detectable after VEGF gene transfer and thus might not reach up to a certain threshold that is needed to induce a significant result [26]. Second, $ApoE^{-/-}$ and $LDLR^{-/-}$ mice on a high-fat diet rarely display IP neovascularization and have significantly lower VEGF levels. Given that these animal models do not mimic the human pathological setting, it is not possible to draw correct conclusions from these models.

Although severe cardiotoxicity rarely occurs in clinical trials using axitinib [28–30], patients on VEGF-inhibiting medication may experience cardiovascular adverse effects [16]. Therefore, cardiac function was also investigated in the present study. Surprisingly, cardiac parameters such as FS, LV mass and cardiomyocyte size were significantly improved in axitinib-treated animals. Moreover, mice displayed less myocardial infarctions and developed less coronary plaques after treatment. Because axitinib inhibits early atherogenesis through downregulation of adhesion molecules and stimulation of VE-cadherin expression (vide supra), we assume that the aforementioned observations in the heart are due to less coronary plaque formation. Unfortunately, we were unable to detect IP neovascularization in coronary arteries of untreated mice due to technical reasons (plaques too small) and also the extent of plaque formation in coronary arteries could not be measured as longitudinal sections of the arteries are necessary to calculate this parameter. Of note, since VEGF is important for capillary density in the myocardium and is associated with contractile dysfunction of the heart, alterations in VEGF plasma levels can cause problems in this particular area (as is seen in certain patients). However, it is likely that short term inhibition of VEGFR signalling in the present study did not lower VEGF levels below a threshold that is necessary to hamper capillary density and thus cardiac dysfunction. Also previous pre(clinical) studies showed that axitinib does not have a negative effect on cardiac function [31–33].

5. Conclusion

Axitinib inhibits IP neovascularization with a subsequent reduction of IP haemorrhages. Axitinib did not change plaque thickness, though plaques showed a more stable phenotype after treatment. Moreover, cardiac function and morphology was improved by axitinib.

Acknowledgements

This work was supported by the University of Antwerp (FFB130136) (DOCPRO-BOF), the Hercules Foundation (AUHA/13/03), the Fund for Scientific Research (G.0412.16N) (FWO) – Flanders and the Horizon 2020 program of the European Union – Marie Skłodowska Curie actions – ITN – MOGLYNET (675527). The authors would like to thank Anne-Elise Van Hoydonck, Cor Van Hove, Hermine Fret, Mart Theunis and Rita Van den Bossche for technical help.

References

[1] P. Libby, Mechanisms of acute coronary syndromes and their implications for therapy, N. Engl. J. Med. 368 (2013) 2004–2013.
[2] R. Virmani, F.D. Kolodgie, A.P. Burke, A.V. Finn, H.K. Gold, T.N. Tulenko, S.P. Wrenn, J. Narula, Atherosclerotic plaque progression and vulnerability to rupture: angiogenesis as a source of intraplaque hemorrhage, Arterioscler. Thromb. Vasc. Biol. 25 (2005) 2054–2061.
[3] B. Van der Veken, G.R. De Meyer, W. Martinet, Intraplaque neovascularization as a novel therapeutic target in advanced atherosclerosis, Expert Opin. Ther. Targets 20 (2016) 1247–1257.
[4] M. Järvilehto, P. Tuohimaa, Vasa vasorum hypoxia: initiation of atherosclerosis, Med. Hypotheses 73 (2009) 40–41.
[5] J.C. Sluimer, J.-M. Gasc, J.L. van Wanroij, N. Kisters, M. Groeneweg, M.D. Sollewijn Gelpke, J.P. Cleutjens, L.H. van den Akker, P. Corvol, B.G. Wouters, M.J. Daemen, A.-P.J. Bijnens, Hypoxia, hypoxia-inducible transcription factor, and macrophages in human atherosclerotic plaques are correlated with intraplaque angiogenesis, J. Am. Coll. Cardiol. 51 (2008) 1258–1265.
[6] J.C. Sluimer, M.J. Daemen, Novel concepts in atherogenesis: angiogenesis and hypoxia in atherosclerosis, J. Pathol. 218 (2009) 7–29.
[7] J.C. Sluimer, F.D. Kolodgie, A.P.J.J. Bijnens, K. Maxfield, E. Pacheco, B. Kutys, H. Duimel, P.M. Frederik, V.W.M. van Hinsbergh, R. Virmani, M.J.A.P. Daemen, Thin-walled microvessels in human coronary atherosclerotic plaques show incomplete endothelial junctions relevance of compromised structural integrity for intraplaque microvascular leakage, J. Am. Coll. Cardiol. 53 (2009) 1517–1527.
[8] J. Pelisek, G. Well, C. Reeps, M. Rudelius, A. Kuehnl, M. Culmes, H. Poppert, A. Zimmermann, H. Berger, H.-H. Eckstein, Neovascularization and angiogenic factors in advanced human carotid artery stenosis, Circ. J. 76 (2012) 1274–1282.
[9] P.R. Moreno, K.R. Purushothaman, V. Fuster, D. Echeverri, H. Truszczynska, S.K. Sharma, J.J. Badimon, W.N. O'Connor, Plaque neovascularization is increased in ruptured atherosclerotic lesions of human aorta: implications for plaque vulnerability, Circulation 110 (2004) 2032–2038.
[10] G.R.Y. De Meyer, D.M.M. De Cleen, S. Cooper, M.W.M. Knaapen, D.M. Jans, W. Martinet, A.G. Herman, H. Bult, M.M. Kockx, Platelet phagocytosis and processing of beta-amyloid precursor protein as a mechanism of macrophage activation in atherosclerosis, Circ. Res. 90 (2002) 1197–1204.
[11] J.L. Van Herck, G.R.Y. De Meyer, W. Martinet, C.E. Van Hove, K. Foubert, M.H. Theunis, S. Apers, H. Bult, C.J. Vrints, A.G. Herman, Impaired fibrillin-1 function promotes features of plaque instability in apolipoprotein E-deficient mice, Circulation 120 (2009) 2478–2487.
[12] C. Van der Donckt, J.L. Van Herck, D.M. Schrijvers, G. Vanhoutte, M. Verhoye, I. Blockx, A. Van Der Linden, D. Bauters, H.R. Lijnen, J.C. Sluimer, L. Roth, C.E. Van Hove, P. Fransen, M.W. Knaapen, A.-S. Hervent, G.W. De Keulenaer, H. Bult, W. Martinet, A.G. Herman, G.R.Y. De Meyer, Elastin fragmentation in atherosclerotic mice leads to intraplaque neovascularization, plaque rupture, myocardial infarction, stroke, and sudden death, Eur. Heart J. 36 (2015) 1049–1058.
[13] M.J. Cross, J. Dixelius, T. Matsumoto, L. Claesson-Welsh, VEGF-receptor signal transduction, Trends Biochem. Sci. 28 (2003) 488–494.
[14] J. Gavard, J.S. Gutkind, VEGF controls endothelial-cell permeability by promoting the beta-arrestin-dependent endocytosis of VE-cadherin, Nat. Cell Biol. 8 (2006) 1223–1234.
[15] M. Inoue, H. Itoh, M. Ueda, T. Naruko, A. Kojima, R. Komatsu, K. Doi, Y. Ogawa, N. Tamura, K. Takaya, T. Igaki, J. Yamashita, T.-H. Chun, K. Masatsugu, A.E. Becker, K. Nakao, Vascular endothelial growth factor (VEGF) expression in human coronary atherosclerotic lesions : possible pathophysiological significance of VEGF in progression of atherosclerosis, Circulation 98 (1998) 2108–2116.
[16] Y. Wasserstrum, R. Kornowski, P. Raanani, A. Leader, O. Pasvolsky, Z. Iakobishvili, Hypertension in cancer patients treated with anti-angiogenic based regimens, Cardio-Oncology 1 (2015) 6.
[17] J. Zhang, Y.-J. Cao, F.-Y. Li, J. Li, L.-B. Yao, E.-K. Duan, Effects of fibronectin, VEGF and angiostatin on the expression of MMPs through different signaling pathways in the JEG-3 cells, Am. J. Reprod. Immunol. 50 (2003) 273–285.
[18] R. Khurana, L. Moons, S. Shafi, A. Luttun, D. Collen, J.F. Martin, P. Carmeliet,

I.C. Zachary, Placental growth factor promotes atherosclerotic intimal thickening and macrophage accumulation, Circulation 111 (2005) 2828–2836.
[19] S.E. Heinonen, A.M. Kivelä, J. Huusko, M.H. Dijkstra, E. Gurzeler, P.I. Mäkinen, P. Leppänen, V.M. Olkkonen, U. Eriksson, M. Jauhiainen, S. Ylä-Herttuala, The effects of VEGF-A on atherosclerosis, lipoprotein profile, and lipoprotein lipase in hyperlipidaemic mouse models, Cardiovasc. Res. 99 (2013) 716–723.
[20] F.L. Celletti, J.M. Waugh, P.G. Amabile, A. Brendolan, P.R. Hilfiker, M.D. Dake, Vascular endothelial growth factor enhances atherosclerotic plaque progression, Nat. Med. 7 (2001) 425–429.
[21] A.D. Hauer, G.H.M. van Puijvelde, N. Peterse, P. de Vos, V. van Weel, E.J.A. van Wanrooij, E.A.L. Biessen, P.H.A. Quax, A.G. Niethammer, R.A. Reisfeld, T.J.C. van Berkel, J. Kuiper, Vaccination against VEGFR2 attenuates initiation and progression of atherosclerosis, Arterioscler. Thromb. Vasc. Biol. 27 (2007) 2050–2057.
[22] J.H.P. Lardenoye, Accelerated atherosclerosis and calcification in vein grafts: a study in APOE*3 Leiden transgenic mice, Circ. Res. 91 (2002) 577–584.
[23] M.R. de Vries, R.C. de Jong, E.A. Peters, J.F. Hamming, M.-J. Goumans, P.H. Quax, Abstract 642: vascular endothelial growth factor receptor 2 blockade in murine vein graft ameliorates lesion growth and enhances plaque stability by reducing intraplaque hemorrhage, Arter. Thromb. Vasc. Biol. 34 (2014) A642.
[24] N. Rahimi, VEGFR-1 and VEGFR-2: two non-identical twins with a unique physiognomy, Front. Biosci. 11 (2006) 818–829.
[25] T.T. Rissanen, J.E. Markkanen, M. Gruchala, T. Heikura, A. Puranen, M.I. Kettunen, I. Kholová, R.A. Kauppinen, M.G. Achen, S.A. Stacker, K. Alitalo, S. Ylä-Herttuala, VEGF-D is the strongest angiogenic and lymphangiogenic effector among VEGFs delivered into skeletal muscle via adenoviruses, Circ. Res. 92 (2003) 1098–1106.
[26] P. Leppänen, S. Koota, I. Kholová, J. Koponen, C. Fieber, U. Eriksson, K. Alitalo, S. Ylä-Herttuala, Gene transfers of vascular endothelial growth factor-a, vascular endothelial growth factor-B, vascular endothelial growth factor-C, and vascular endothelial growth factor-D have no effects on atherosclerosis in hypercholesterolemic low-density lipoprotein, Circulation 112 (2005).
[27] S. Winnik, C. Lohmann, G. Siciliani, T. von Lukowicz, K. Kuschnerus, N. Kraenkel, C.E. Brokopp, F. Enseleit, S. Michels, F. Ruschitzka, T.F. Lüscher, C.M. Matter, Systemic VEGF inhibition accelerates experimental atherosclerosis and disrupts endothelial homeostasis – implications for cardiovascular safety, Int. J. Cardiol. 168 (2013) 2453–2461.
[28] O. Rixe, R.M. Bukowski, M.D. Michaelson, G. Wilding, G.R. Hudes, O. Bolte, R.J. Motzer, P. Bycott, K.F. Liau, J. Freddo, P.C. Trask, S. Kim, B.I. Rini, Axitinib treatment in patients with cytokine-refractory metastatic renal-cell cancer: a phase II study, Lancet Oncol. 8 (2007) 975–984, http://dx.doi.org/10.1016/S1470-2045(07)70285-1.
[29] H.S. Rugo, R.S. Herbst, G. Liu, J.W. Park, M.S. Kies, H.M. Steinfeldt, Y.K. Pithavala, S.D. Reich, J.L. Freddo, G. Wilding, Phase I trial of the oral antiangiogenesis agent AG-013736 in patients with advanced solid tumors: pharmacokinetic and clinical results, J. Clin. Oncol. 23 (2005) 5474–5483.
[30] B.I. Rini, T. de La Motte Rouge, A.L. Harzstark, M.D. Michaelson, G. Liu, V. Grünwald, A. Ingrosso, M.A. Tortorici, P. Bycott, S. Kim, J. Bloom, R.J. Motzer, Five-year survival in patients with cytokine-refractory metastatic renal cell carcinoma treated with axitinib, Clin. Genitourin. Cancer 11 (2013) 107–114.
[31] G.G. Hillman, F. Lonardo, D.J. Hoogstra, J. Rakowski, C.K. Yunker, M.C. Joiner, G. Dyson, S. Gadgeel, V. Singh-Gupta, Axitinib improves radiotherapy in murine xenograft lung tumors, Transl. Oncol. 7 (2014) 400–409.
[32] S. Bracarda, D. Castellano, G. Procopio, J.M. Sepúlveda, M. Sisani, E. Verzoni, M. Schmidinger, Axitinib safety in metastatic renal cell carcinoma: suggestions for daily clinical practice based on case studies, Expert Opin. Drug Saf. 13 (2014) 497–510.
[33] M. gross-goupil, L. Francois, A. Quivy, A. Ravaud, Axitinib: a review of its safety and efficacy in the treatment of adults with advanced renal cell carcinoma, Clin. Med. Insights Oncol. (2013) 269.